X_{cp} and X_{cg} are distances from origin 0 to the center of pressure, and the center of gravity, respectively. M is the total mass of structure. $\overline{C_{N_\alpha} S}$ is the product of total normal force coefficient slope and total reference area; q is dynamic pressure; $\rho_{r,n}$ is the total slope influence coefficient (slope at $X = X_r$ is due to a unit load at $X = X_n$ when cantilevered at $X = 0$); and p is the total number of discrete elements of discrete mass representation of the structure.

It is found that matrix $[A]$ of Eq. (2) is a numerically invariant quantity regardless of the location of the reference point 0. The proof of the preceding statement is as follows. Reference 1 selects the reference station at one of the discrete masses by virtue of which the matrix size will be reduced by one less than the number of discrete stations comprising the discrete mass system. Let us take a new reference station at a distance a from previous reference station 0. Then new X_r', the distance of rth station from the new reference station 0′ in terms of X_r is related by

$$X_r' = X_r - a$$

or, in general,

$$\{X_r'\} = \{X_r - a\}$$

It is seen that

$$X_{cg}' - X_{cp}' = X_{cg} - X_{cp} = \text{constant} \tag{3a}$$

$$X_{cp}' - X_r' = X_{cp} - X_r \tag{3b}$$

$$X_r' - X_{cg}' = X_r - X_{cg} \tag{3c}$$

$$\overline{C_{N_\alpha} S'} = \overline{C_{N_\alpha} S} = \sum_{r=1}^{p-1} C_{N_\alpha} S_r + C_{N_\alpha} S_o \tag{3d}$$

$$M' = M = \sum_{r=1}^{p-1} m_r + m_o \tag{3e}$$

Equations (3d) and (3e) are the sum of product of normal force-coefficient slope and panel areas of all stations; and total mass of structure, respectively, and are independent of the reference coordinate system.

The transformation matrix computed by selecting a new reference station at 0′ (let us denote it by $[A']$) is given as

$$[A'] = \left[[1] + \left\{ \frac{m_r}{M} \right\} \left[\frac{X_{cp}' - X_r'}{X_{cg}' - X_{cp}'} \right] + \left[\frac{C_{N_\alpha} S_r}{\overline{C_{N_\alpha} S}} \right] \{1\} \times \left[\frac{X_r' - X_{cg}'}{X_{cg}' - X_{cp}'} \right] \right]$$

Using Eq. (3)

$$[A'] = [A] \tag{4}$$

is the same as transformation matrix $[A]$ of Eq. (2), which is obtained by taking the reference station at 0. Thus, the transformation matrix $[A]$ is a numerically invariant quantity regardless of the location of the reference point 0.

This is because the transformation matrix $[A]$ is obtained by using the translational and rotational equilibrium conditions

$$[1]\{F_r\} + F_o = 0$$

and

$$[X_r]\{F_r\} = 0$$

respectively, and which does not depend on the coordinate system used for formulation.

Now with respect to the new reference station at 0′, Eq. (1) is written as

$$\{F_n'\} = q\overline{C_{N_\alpha} S}[A'] \left[\frac{C_{N_\alpha} S_r}{\overline{C_{N_\alpha} S}} \right] [\rho_{r,n}'] \{F_n'\} \tag{5}$$

where $\rho_{r,n}'$ is the total slope influence coefficient with respect to the new reference station 0′.

Using Eq. (4) in Eq. (5)

$$\{F_n'\} = q\overline{C_{N_\alpha} S}[A] \left[\frac{C_{N_\alpha} S_r}{\overline{C_{N_\alpha} S}} \right] [\rho_{r,n}'] \{F_n'\} \tag{6}$$

Equations (1) and (6) represent eigenvalue problem for a given structure using different coordinate systems, hence, will yield the same eigenvalues. The eigenvectors, in general, will represent the normalized mode shape with reference to the coordinate system used in the formulation. It is seen from Eqs. (1) and (6) that matrix $[A]$ computed at reference station 0 can be used together with the matrix of slope influence coefficients $[\rho_{r,n}]$, computed at either reference station 0 or 0′. Since $[A]$ is a numerically invariant quantity regardless of reference coordinate system, matrix $[A]$ computed at any point can be used in Eq. (1) together with any set of slope influence coefficients for the structure clamped at any other point. For the structure clamped at the Sth station $\rho_{r,n} = 0$ for $r \leqq S \leqq n$.

Proper choice of S will reduce considerably the amount of computations for the $\rho_{r,n}$'s. Note that matrix $[A]$ has to be calculated by suppressing the Sth row and column since the structure is clamped at the Sth discrete mass.

It is also seen that matrix $[A]$ can be very easily calculated choosing the reference station at center of gravity of the structure. Then the expression for $[A]$ simplifies to

$$[A] = \left[[1] - \left\{ \frac{m_r}{M} \right\} [1] + \left\{ \frac{m_r}{M} - \frac{C_{N_\alpha} S_r}{\overline{C_{N_\alpha} S}} \right\} \left[\frac{X_r}{X_{cp}} \right] \right]$$

Note that then the X_r's are measured from the center of gravity as the reference station.

In the past, Refs. 2, 3 have shown the numerical invariance of similar transformation matrix in the case of vibration analysis of free-free structures. Reference 2 uses a lumped mass representation of the structure, whereas Ref. 3 uses a modified mass matrix method (then the mass matrix is full rather than a diagonal one as in the case of the lumped mass method). The way of formulation in all cases[1-3] is the same. Hence, in general, it is concluded here that if the formulation of the problem using matrix notations is done in the way given in Refs. 1–3, then the corresponding transformation matrix obtained for free-free structures would always be a numerically invariant quantity regardless of the location of the reference point.

References

[1] Alley, V. L. and Gerringer, A. H., "An Analysis of Aeroelastic Divergence in Unguided Launch Vehicles," TND-3281, March 1966, NASA.

[2] Dugundji, J., "On the Calculation of Natural Modes of Free-Free Structures," *Journal of Aero-Space Sciences*, Vol. 28, No. 2, Feb. 1961, pp. 164–165.

[3] Durvasula, S., Humbad, N. G., and Nair, P. S., "Vibration of Slender Rocket Vehicles," *Proceedings of the Second Symposium on Space Science and Technology*, Rocket Society of India, Sept. 1973.

Experimental Study of Mixed Convection Heat Transfer in an MHD Channel

H. K. YANG* AND C. P. YU†
State University of New York at Buffalo, Buffalo, N.Y.

Nomenclature

a = width of the channel
b = depth of the channel

Received January 24, 1974; revision received August 5, 1974. Presented as Paper 74-510 at the AIAA 7th Fluid and Plasma Dynamics Conference, Palo Alto, Calif., June 17–19, 1974. The authors are grateful to W. Schulze for constructing part of the equipment. This research was supported in part by the State University of New York Research Foundation.

Index category: Plasma Dynamics and MHD.

* Graduate Student; now Technical Staff, General Electric Co., Sunnyvale, Calif. Member AIAA.

† Professor, Department of Engineering Science, Faculty of Engineering and Applied Science. Member AIAA.

B_o = applied magnetic field
$\dot{C}_M$ = time rate of heat capacity of mercury
$\dot{C}_W$ = time rate of heat capacity of water
D_e = equivalent diameter, $(2ab/a+b)$
g = gravitational acceleration
Gr = Grashof number, $\beta q D_e^4 \bar{q}/Kv$
h = over-all heat transfer coefficient
K = thermal conductivity
M = Hartmann number, $B_o D_e(\sigma/\mu)^{1/2}$
$\bar{q}$ = average heat flux per unit area
Re = Reynolds number, VD_e/v
S = total heat exchange surface area
T_M = mercury temperature
T_{MI} = mercury temperature at the inlet
T_{MO} = mercury temperature at the outlet
T_W = water temperature
V = mean axial velocity
β = thermal expansion coefficient
μ = absolute viscosity
v = kinematic viscosity
σ = electrical conductivity

I. Introduction

WHEN an electrically conducting fluid flows in a duct, the effects of an imposed transverse magnetic field, in general, are twofold. First, the velocity of the fluid close to the walls is smaller than that at the center; the Lorentz force thus tends to retard the flow in the central part and to accelerate it (or retards it to a lesser degree if the wall is electrically conducting) near the walls. Therefore, the velocity profile is flattened. This is usually called the Hartmann effect. Secondly, the magnetic field has a stabilizing effect on the flow and suppresses turbulent fluctuations. The consequence of this effect is a reduction of the skin friction in the turbulent flow and an increase in the laminar flow. This phenomenon has been used by many authors for determining the condition where the transition from turbulent to laminar takes place.

Murgatroyd[1] first observed this transition point in a mercury channel flow in a transverse magnetic field and found that the transition appears approximately at $Re/M = 225$. This result was later derived analytically by Lykoudis[2] based on the comparison of the Hartmann profile with the logarithmic turbulent velocity profile. Further detailed measurements and theory[3,4] by Lykoudis and Brouillette have confirmed this result.

Experimental results of MHD forced convection heat transfer in a duct in the turbulent flow regime have become available in the past few years.[5-9] These authors showed that at large Reynolds numbers, where convection mechanism predominates, the magnetic field inhibits heat transfer. In the laminar flow region, however, no experimental data have been published. This is because liquid metals usually used in the experiment have small Prandtl number. In the laminar flow region, heat transfer is dominated by conduction mechanism. The change of convection pattern in the laminar case has only a relatively minor effect on total heat transfer. Theoretical calculation, however, shows an increase of heat transfer in the laminar flow regime.[10] In this study, an experiment on heat transfer of the combined forced and free convection flow in a vertical mercury-water heat exchanger under the influence of a transverse magnetic field is made. The over-all heat transfer is measured in both laminar and turbulent flow regimes.

II. Experimental Arrangement

The basic design of the mercury flow system is shown schematically in Fig. 1. The system was completely closed and airtight. The flow through the test section was generated by a head difference, which could be controlled. This is desirable in order to remove the disturbance and pulsation generated by direct pumping. The pump was operated at a higher capacity of flow than that flowing through the test section. The rest of flow was by-passed through an overflow pipe connected to a sump tank. In order to equalize the vapor pressure which may build up during pumping, a vent pipe was connected between the head tank and the sump tank. The loop, with the exception of the test section, was made from steel pipe and fittings.

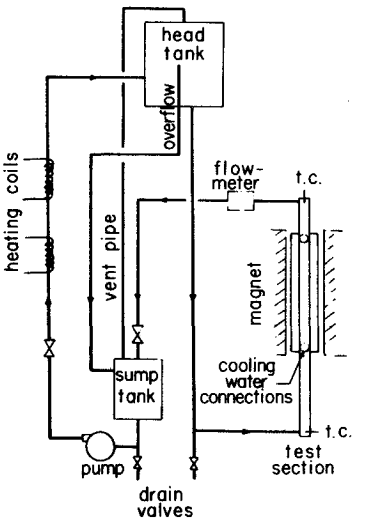

Fig. 1 Diagram of the mercury flow system.

Mercury flow rate was measured by an electromagnetic flow meter which was mounted in the piping system. The electric potential output was fed to a null meter. The flow meter was calibrated by timing the filling of a tank of known volume with mercury.

The electromagnet with a d.c. power supply was capable of producing a maximum field of 18,000 gauss at 65 amp. The dimensions of the pole faces area were 18 in. long by $2\frac{1}{2}$ in. wide and 1 in. gap. A calibration with a Bell 120 gauss meter showed that the magnetic field strength along the gap was constant within 1% until about $\frac{1}{2}$ in. to the ends. The variation in the horizontal direction was too small to be measured.

The test section is shown in Fig. 2. It was constructed with 304 stainless steel tubing. The inner surface was not coated for electrical insulation. The water jacket and two mixing chambers were welded together with the mercury channel. The channel had the dimensions of 1.40 in. × 0.40 in. i.d., 16 in. long with an additional 12 in. hydraulic entrance length and 0.050 in. wall thickness. The water jacket outside dimensions were $1\frac{7}{8}$ in. × $\frac{7}{8}$ in. The size of the channel was designed as large as it could be to fit into the gap of the electromagnet in order to obtain maximum natural convection. The channel and water jacket were placed at the middle of the gap space.

The mercury was heated before entering the test section by heating coils along the pipe from the pump to the head tank. The coils were separated into several units and heated independently to achieve different heating rates. Cooling water was pumped from a reservoir tank to give a better steady-state flow. The water passed a flow meter and the rate was controlled by a valve.

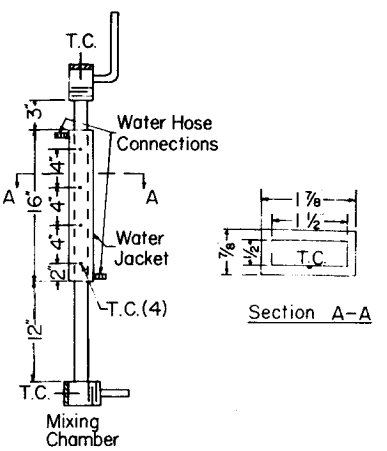

Fig. 2 Test section.

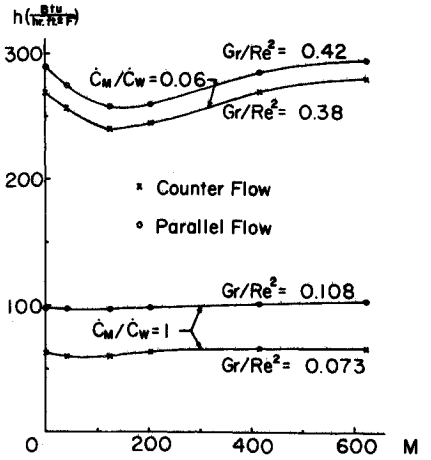

Fig. 3 Over-all heat transfer coefficient vs M for $Re = 11{,}000$ and different flow conditions.

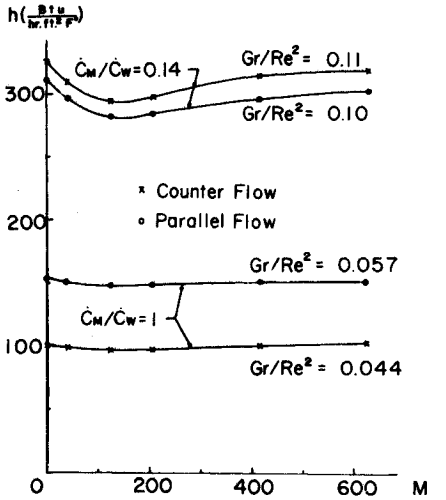

Fig. 4 Over-all heat transfer coefficient vs M for $Re = 25{,}000$ and different flow conditions.

The thermocouples at the inlet and outlet of mercury and water were connected to a rotary switch. The outputs were measured by a potentiometer and were recorded. Portions of the test section from the mixing chambers to the water jacket were covered with thermal insulating material to reduce heat loss at that part and thus increase the accuracy of true mercury inlet and outlet bulk temperature.

III. Results

Data were obtained for $Re = 11{,}000$ and 25,000 at magnetic fields of 0, 1, 3, 5, 10, and 15 kilogauss and different mercury and water flow conditions. The heated mercury flowed upward while the cooling water flowed in either counter-flow or parallel-flow direction. The tests with the magnetic field on were conducted alternatively with the zero-field test so the results with the magnetic field on can compare directly with those of the zero-field case. The general characteristic parameters of the experiment are given in Table 1.

The mercury and water inlet and outlet bulk temperature are used to calculate the over-all heat transfer coefficient, following the relation.[11]

$$h = \bar{q}\,\frac{\ln(T_M - T_W)_1 - \ln(T_M - T_W)_2}{(T_M - T_W)_1 - (T_M - T_W)_2} \qquad (1)$$

where the subscripts 1 and 2 denote the two ends of the heat exchanger and $\bar{q} = \dot{C}_M/S(T_{MI} - T_{MO})$ is the average heat flux per unit area, in which $\dot{C}_M$ is the time rate of heat capacity (flow rate times specific heat) of the mercury and S is the surface area of heat exchange.

The over-all heat transfer coefficient h is plotted against M in Figs. 3 and 4. Since an applied magnetic field has no effect on the water flow, the net change of heat transfer comes from the mercury side. Applying the field first reduces the heat transfer in mercury by suppressing turbulent fluctuations and free convection. Then, as the field increases further, the flow becomes laminar and the Hartmann effect takes over the dominant role, so the heat transfer is increased.

This dual effect on heat transfer by the magnetic field which is not observable in forced convection liquid metal MHD channel, as stated above, becomes apparent when free convection is present. The effect is more noticeable when free convection becomes greater, or Gr is larger, as shown in Figs. 3 and 4. What happens physically in this case is that the magnetic field seems to inhibit free convection heat transfer more effectively than turbulence suppression effect; the decrease of heat transfer by the magnetic field appears more profound in the turbulent flow regime. As the magnetic field becomes very large, free convection is less important in the laminar flow and heat transfer increases due to the Hartmann effect.

Figure 5 presents the values of Re/M for the minimum point of heat transfer based upon the measurements shown in Figs. 3 and 4. It is seen that Re/M decreased with increasing Gr/Re^2. It is not clear what physical situation this minimum point is corresponding to. Presumably, it is an indication of the transition from the turbulent to laminar flow when the free convection is present. Figure 5 shows that the appearance of the free convection, particularly with higher temperature at the lower side, tends to promote or amplify the turbulent fluctuations in the flow, and a large magnetic field is needed in order to completely suppress them. The results of Re/M may be extrapolated to the case $Gr = 0$, yielding $Re/M \cong 225$ in the absence of free convection. A straight line extrapolation gives $Re/M = 217$. The value agrees well with the results of the transition point from turbulent to laminar flow based upon the skin friction measurements.

Table 1 Design parameters

Channel Dimensions	
Cross section (i.d.)	1.40 in. × 0.40 in.
Test section length	16 in.
Hydraulic entrance length	12 in.
Equivalent diameter	0.62 in.
Reynolds number	11,000 and 25,000
Hartmann number	0–620
Grashof number	8.8×10^6–6.8×10^7
Mercury flow rate	0.4 and 0.9 gpm
Water flow rate	0.2–30 gpm
Mercury inlet temperature	100°F–150°F
Water inlet temperature	42°F–52°F
Mercury temperature change (T_{MI}–T_{MO})	10°F–70°F
Water temperature change (T_{WO}–T_{WI})	4°F–30°F

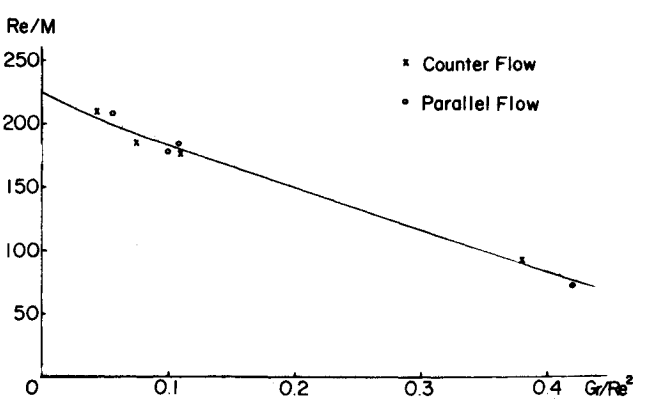

Fig. 5 Values of Re/M at the minimum point of heat transfer vs Gr/Re^2.

Finally, it must be pointed out that in this experiment the hydraulic entrance length was about 19 hydraulic diameters. At higher Reynolds number flow than we have considered here, a longer entrance length is needed to achieve fully developed turbulent flow.[3] Furthermore, Eq. (1) is derived by neglecting the magnetic and thermal entrance effects; local heat transfer coefficient measurements are needed in future research to justify this assumption.

References

[1] Murgatroyd, W., "Experiments on Magneto-Hydrodynamic Channel Flow," *Philosophy Magazine*, Vol. 44, No. 359, Dec. 1953, pp. 1348–1354.

[2] Lykoudis, P. S., "Transition from Laminar to Turbulent Flow in Magneto-Fluid Mechanic Channels," *Review of Modern Physics*, Vol. 32, No. 4, Oct. 1960, pp. 796–798.

[3] Brouillette, E. C. and Lykoudis, P. S., "Magneto-Fluid-Mechanic Channel Flow. I. Experiment," *The Physics of Fluids*, Vol. 10, No. 5, May 1967, pp. 995–1001.

[4] Lykoudis, P. S. and Brouillette, E. C., "Magneto-Fluid-Mechanic Channel Flow. II. Theory," *The Physics of Fluids*, Vol. 10, No. 5, May 1967, pp. 1002–1007.

[5] Gardner, R. A., Uherka, K. L., and Lykoudis, P. S., "The Influence of a Transverse Magnetic Field on Forced Convection Liquid Metal Heat Transfer," *AIAA Journal*, Vol. 4, No. 5, May 1966, pp. 848–852.

[6] Krasilnikov, E. Y., "The Effect of a Transverse Magnetic Field upon Convective Heat Transfer in Magnetohydrodynamic Channel Flows," *Magnitnaya Gidrodinamika*, Vol. 1, No. 3, March 1965, pp. 37–40.

[7] Kovner, D. S., Krasilnikov, E. Y., and Danevin, J. G., "Experimental Study of the Effect of a Longitudinal Magnetic Field on Convective Heat Transfer in a Turbulent Tube Flow of Conducting Liquid," *Magnitnaya Gidrodinamika*, Vol. 2, No. 4, April 1966, pp. 101–106.

[8] Krasilnikov, E. Y., "A Study of the Effect of a Magnetic Field on Convective Heat Transfer in a Turbulent Flow of an Electrically Conducting Fluid in Channels," dissertation, Moscow Power Engineering Institute, Moscow, USSR, 1966.

[9] Gardner, R. A. and Lykoudis, P. S., "Magneto-Fluid-Mechanic Pipe Flow in a Transverse Magnetic Field, Part 2. Heat Transfer," *Journal of Fluid Mechanics*, Vol. 48, Pt. 1, Jan. 1971, pp. 129–141.

[10] Hwang, C. L., Knieper, P. J., and Fan, L. T., "Heat Transfer to MHD Flow in the Thermal Entrance Region of a Flat Duct," *International Journal of Heat and Mass Transfer*, Vol. 9, No. 6, June 1971; pp. 773–789.

[11] Jacob, M., *Heat Transfer*, Vol. 2, Wiley, New York, 1963, p. 206.

Three-Dimensional Laminar Boundary Layer over a Body of Revolution at Incidence and With Separation

W. GEISSLER*

Deutsche Forschungs- und Versuchsanstalt für Luft- und Raumfahrt E.V. Aerodynamische Versuchsanstalt Göttingen, F.R. Germany

Nomenclature

x, r = cylindrical coordinates
L = total length of body
ξ, η, ζ = system of rectangular coordinates, oriented with regard to the potential flow
ξ = in direction of streamlines
η = in direction of equipotential lines
ζ = normal to body surface
S = stagnation point of potential flow
U = velocity of potential flow
U_m = meridional component of U
U_ϕ = circumferential component of U
U_∞ = velocity of undisturbed flow
α = angle of incidence of the body

Received March 4, 1974; revision received July 26, 1974. This Note is a very condensed version of the author's paper[8] which will shortly be published in German.

Index category: Boundary Layers and Convective Heat Transfer—Laminar.

* Research Scientist.

Introduction

THE exact prediction of the position of boundary-layer separation for bodies at angle of attack is a problem of great practical importance in aircraft design. Boundary-layer calculations based on one of the common simplifications such as similarity, small crossflow, small perturbation give only approximate solutions of this problem which are not always satisfactory. In the present method, no simplification of the boundary-layer equations is introduced. The complete three-dimensional laminar boundary-layer equations are solved numerically by an implicit finite difference technique.

Recently, Blottner and Ellis[1] and Wang[2] also presented methods based on finite difference concepts. A discussion of separation patterns over inclined bodies of revolution was given by Wang.[3] Both authors use coordinate systems which are fixed to the body geometry. To extend the calculation over the entire body surface a separate quasi two-dimensional calculation process along one line of symmetry is necessary to specify initial boundary-layer profiles along this line. The application of both methods is limited to simple bodies of revolution like prolate spheroids or elliptic-paraboloids where the inviscid flow data can be obtained analytically.

In the present method a streamline coordinate system is introduced. The coordinates are represented by the streamlines and potential lines of the outer inviscid flow. Using streamline coordinates the extension of the numerical boundary-layer calculation over the entire body surface is a straightforward process. No transformation from one into another coordinate system is necessary. A finite difference scheme is chosen which permits one to include the lines of symmetry of the flow into the calculation process. No initial data along the lines of symmetry have to be specified. The outer inviscid flow is calculated numerically by a singularity method which has been developed by the author.[4] Therefore this method is applicable to bodies of revolution with arbitrary cross-sections. To determine the position of boundary-layer separation the condition of numerical stability (Courant-Friedrich-Levy condition) serves as a useful criterion.

Governing Equations

Figure 1 describes the problem and gives the notation in a streamline coordinate system: the rectilinear coordinate system ξ, η, ζ is oriented in the direction of streamlines, equipotential lines, and normal to the surface, respectively. The corresponding velocity components in these directions are, u, v, w, whereas U is the velocity of the outer inviscid flow, U_∞ is the undisturbed mainflow velocity, and α the angle of attack. Here the velocity component u, which is parallel to the streamlines of the outer flow, is the primary velocity and the velocity component v normal to the streamlines gives the secondary flow in the boundary layer. All lengths are made dimensionless with the

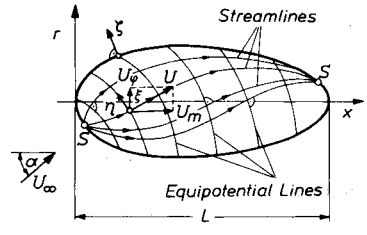

Fig. 1 Flow around a body of revolution at incidence.